On the Impact of the Grid on the Synchronization Stability of Grid-Following Converters

Junru Chen, *IEEE Member*, Wenjia Si, Muyang Liu, *IEEE Member*, Federico Milano, *IEEE Fellow*

***Abstract*—The research on the synchronization stability of Grid-Following Converter (GFL) is of great significance for the stable operation of inverter-based resources. Existing literature mainly focuses the stability factors from the point of view of the converter and assumes the grid to be an infinite-bus with constant frequency. However, faults cause the grid to experience interdependent variations of grid voltage amplitudes and phases, as well as of its frequency. The impact of these variations on the synchronization stability has not been systematically and comprehensively studied yet. Here we study the combined effect on GFL synchronization stability of all these quantities following a large disturbance. The theoretical appraisal shows that phase-angle jump affects the initial perturbance of the GFL while the grid frequency affects the following transient responses and the stability boundary. Simulation results also show that the variation of the frequency with higher RoCoF may be beneficial for the stability of the GFL, and that the effects of the various of the voltage and frequency can be studied separately.**

Keywords—Synchronization stability, Phase-Locked Loop (PLL), phase-angle jump, frequency variation, combined grid-disturbance

I. INTRODUCTION

Grid-Following converters (GFLs) based on Phase-Locked Loops (PLLs) are a common grid-interface for renewable generation. In a weak grid with high impedance, the loss of the synchronization has been reported to be the main cause for the GFL instability after a severe fault on the grid [1]. This instability may continue even with a sufficient reactive power compensation and even after the fault clearance [2]. In this context, the synchronization stability of GFLs has attracted a great attention in recent years [3]. A Quasi-Static Large-Signal (QSLS) model has been proposed to reflect the transient response of the GFL with respect to the grid fault [4]. Based on the QSLS model, the Equal Area Criterion (EAC) method [5], phase portrait method [6] and Lyapunov function method [7] have been proposed to assess the synchronization stability. Amongst these methods, EAC method can visually show the GFL operating point movement while the phase portrait method can precisely present the GFL stable operational region.

In the literature, the synchronization stability analysis of the GFL focuses on the "converter" itself such as analyzing the effect of the converter inherent controls and the PLL settings, while the "grid" is assumed to be an infinite-bus. However, the synchronization instability of GFL is ultimately caused by grid disturbances. Thus, the effect of the dynamic behavior of the "grid" on the synchronization stability requires a systematic and comprehensive study, which to the best of the authors' knowledge is currently missing. In the literature, in fact, grid disturbances are modelled either as a voltage sag or as a short-circuit, i.e., voltage sag plus phase angle jump. Frequency variations, which are also common after the occurrence of a fault, are not considered. To cover this gap, in this letter, we present a systematic analysis on the "grid" disturbances, that is, we consider the variation of all grid[1] voltage parameters (magnitude, phase angle, and frequency) both independently and combined. The GFL synchronization stability analysis is carried out both qualitatively, through the EAC and phase portrait method, and quantitatively, though a comprehensive set of simulations.

II. SYNCHRONIZATION STABILITY ANALYSIS

The synchronization stability is referred to as the ability of the GFL to sustain the synchronization after subjecting a large disturbance. The analysis of the transient of the GFL is generally based on the QSLS model as detailed in [4], as follows. The PLL locks the phase at the Point of the Common Coupling (PCC), of which dynamics can be represented as:

$$\begin{cases} \dfrac{d(\delta)}{dt} = \Delta\omega_{pll}, \\ \dfrac{d\Delta\omega_{pll}}{dt} = k_{p,pll}\dfrac{dv_q}{dt} + k_{i,pll}v_q, \end{cases} \tag{1}$$

where $\delta = \theta_{pll} - \theta_g$, θ_{pll} is the phase of the PCC voltage, θ_g is the phase of the grid voltage, ω_g is the frequency of grid voltage, ω_n is the nominal frequency, $k_{p,pll}/k_{i,pll}$ is the PI coefficient of the synchronous reference frame (SRF)-PLL. In a weak grid with a significant grid impedance, the PCC voltage $\boldsymbol{V}_{pcc}$ is no longer constant but varies with the GFL output current as indicated following:

$$\boldsymbol{V}_{pcc} = \boldsymbol{V}_g + \boldsymbol{I}(Z_l + Z_g) \tag{2}$$

Where $\boldsymbol{V}_g$ is the grid voltage, $\boldsymbol{Z}_l$ is the line impedance, $\boldsymbol{Z}_g$ is the grid impedance, $\boldsymbol{I}$ is the GFL output current. Assuming that the PCC voltage is the reference with the phase at 0 rad, then the PCC voltage in the q-axis in the synchronous dq-frame can be obtained as follows:

$$v_q = (r_l + r_g)i_q + (\omega_n + \Delta\omega_{pll})(l_l + l_g)i_d - V_g\sin(\delta) \tag{3}$$

Equations (1)-(3) define the synchronization of the QSLS model of the GFL and are illustrated in Fig. 1. We utilize these equations to deduce the stability region. Based on the grid synchronization loop, the GFL output current flowing in the inductance $l_l + l_g$ introduces a positive-feedback into the synchronism.

---

[1] This work was supported in part by the Science and Technology Department of Xinjiang under the grant No. 2021D01C086.

J. Chen, W. Si and M. Liu are with the School of Electrical Engineering, Xinjiang University, Urumqi, China (e-mail: junru.chen@xju.edu.cn; wenjia_si@stu.xju.edu.cn; muyang.liu@xju.edu.cn).

F. Milano is with the School of Electrical and Electronics Engineering, University College Dublin, Dublin, Ireland (e-mail: federico.milano@ucd.ie).

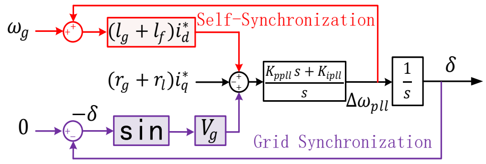

Fig. 1 Quasi-Static Large-Signal model of synchronization stability analysis.

In the literature, "large disturbances" have been classified into the two main following scenarios: (i) *voltage sag*: the grid voltage amplitude V_g step reduces; and (ii) *short-circuit fault*: the grid impedance $\boldsymbol{Z}_g$ changes with respect to the short-circuit impedance, which could be equivalent to $V_g e^{j\theta_g} + Z_g I e^{j(\delta + \angle Z_g)}$ that the equivalent grid voltage changes with respect to both the amplitude and phase.

According to the classification above, grid faults can be actually study in the same framework, i.e., they can be unified as an equivalent voltage (phase) change at the receiving terminal of the line impedance from the GFL. Existing literature emphasizes the analysis of this voltage change on the synchronous transients. In reality, however, not only the voltage but also the frequency changes during the fault. The remainder of the paper analyses the effect of realistic disturbances on the synchronization stability.

III. Effect Of Grid State Variation On Synchronization Stability

Let us assume that the initial grid equivalent voltage is $V_{g,0}\angle(\omega_{g,0}t + \theta_{g,0})$. After the occurrence of the grid fault, the voltage changes, say $(V_{g,0} + \Delta V_g)\angle((\omega_{g,0} + \Delta\omega_g)t + \theta_{g,0} + \Delta\theta_g)$. Substituting the perturbed voltage into (2) leads to:

$$v_q = (V_{g,0} + \Delta V_g)\sin(\Delta\omega_g t + \Delta\theta_g - \delta) + r_g i_q + +\omega_{pll} l_g i_d \quad (4)$$

In a grid fault, the equivalent grid voltage amplitude in general changes, the dynamics of which have been discussed in [5]. We use a phase portrait method to analyze the effect of the grid voltage variations on the synchronization stability. The phase of the PLL θ_{pll} cannot step change due to its integral feature, while the PLL frequency could have a sudden change due to the proportional channel from the input of the PCC voltage. After a voltage magnitude sag, the resulting perturbance for the PLL dynamics (1) is $(\delta_{s,0}, \Delta\omega_{pll@V_g}(t_0^+))$ in the phase plane, where:

$$\delta_{s,0} = sin^{-1}\left(\frac{\omega_g l_g i_d + r_g i_q}{V_{g,0}}\right) \quad (5)$$

$$\Delta\omega_{pll@V_g}(t_0^+) = \frac{k_{p,pll}\Delta V_g \sin(-\delta_{s,0})}{1 - k_{p,pll} l_g i_d} \quad (6)$$

and i_d/i_q is the GFL current in the synchronous d-q frame, r_g/l_g is the grid impedance, $\delta_{s,0}$ is the initial phase before the voltage sag. $\Delta\omega_{pll@V_g}(t_0^+)$ is the PLL frequency at the instant of the grid voltage sag. If this point falls within the stability region, the GFL is stable.

A. Effect of phase-angle jumps

A phase-angle jump does not change the stability region of the GFL. This is easy to see as the grid voltage phase angle does not appear in the QSLS model. However, a phase-angle jump leads to a sudden step change of the phase of the PCC voltage θ_{pll}. Referring to the EAC method in Fig. 2(a), the phase-angle jump leads to the operating point move horizontally and vary the acceleration area. This leads to modify the stability margin of the GFL. Figure 2(b) shows that the phase-angle jump shifts horizontally the initial point by $-\Delta\theta_g$. Moreover, the phase jump can lead to a sudden change of the PLL frequency and shift vertically the initial point by $\Delta\omega_{pll@\theta_g}(t_0^+)$, where:

$$\Delta\omega_{pll@\theta_g}(t_0^+) = \frac{k_{p,pll}(V_{g,0}+\Delta V_g)[\sin(\Delta\theta_g - \delta_{s,0}) - \sin(-\delta_{s,0})]}{1 - k_{p,pll} l_g i_d}. \quad (7)$$

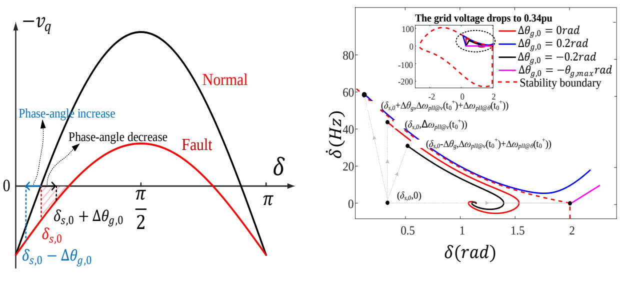

(a) EAC (b) phase-plane diagram

Fig. 2 Effect of the Phase-angle jump.

From the EAC analysis, in the range of $[0, \Delta\theta_{g,max}]$, the larger the negative phase jump $\Delta\theta_g$, the better the GFL synchronous response, where $\Delta\theta_{g,max} = \pi - \frac{\omega_g l_g i_d + r_g i_q}{V_{g,0} + \Delta V_g} - \frac{\omega_g l_g i_d + r_g i_q}{V_{g,0}}$. Otherwise, the phase would jump over the unstable equilibrium point δ_u and fall into the unstable region. From the phase portrait analysis, after the grid fault, the phase jump $\Delta\theta_g$ moves the initial point from $(\delta_{s,0}, \Delta\omega_{pll@V_g}(t_0^+))$ to $(\delta_{s,0} - \Delta\theta_g, \Delta\omega_{pll@\theta_0}(t_0^+) + \Delta\omega_{pll@V_g}(t_0^+))$ but does not affect the stability boundary.

B. Effect of frequency variations

The frequency changes with the slope of rate of change of frequency (RoCoF), which is a function of time, of which maximum rate is restricted by the transmission system operator (TSO), e.g., ±4 Hz/s commanded by Irish TSO, EirGrid. Then, after the faults, the grid frequency in (3) becomes.

$$\Delta\dot{\omega}_g = RoCoF(t) \quad (8)$$

Substituting (8) into (2) and rewriting (1) obtains:

$$\begin{cases} \dfrac{d\delta}{dt} = \Delta\omega_{pll} - \Delta\omega_g, \\ \dfrac{d\Delta\omega_g}{dt} = RoCoF(t), \\ \dfrac{d\Delta\omega_{pll}}{dt} = \dfrac{k_{p,pll}(\Delta\omega_g - \Delta\omega_{pll})V_g cos\delta}{1 - k_{p,pll} l_g i_d} + \\ \qquad + \dfrac{k_{i,pll}(r_g i_q + (\omega_n + \Delta\omega_{pll}) l_g i_d - V_g sin\delta)}{1 - k_{p,pll} l_g i_d} \end{cases} \quad (9)$$

where it appears that the grid frequency change affects the transients of both $\Delta\omega_{pll}$ and δ. The smaller $\int_{t_0^+}^{t}(\Delta\omega_{pll} - \Delta\omega_g)$, the smaller the phase movement and the better the synchronization transients. At one aspect, after the fault occurrence, the PLL frequency from $\Delta\omega_{pll@V_g}(t_0^+)$ is controlled to track $\Delta\omega_g$, while $\Delta\omega_g$ influences the tracking speed of $\Delta\omega_{pll}$, i.e. $\frac{k_{p,pll}\Delta\omega_g V_g cos\delta}{1-k_{p,pll}l_g i_d}$ in (9); At another aspect, $\Delta\omega_g$ changes at the rate of $RoCoF(t)$. If the incremental $\frac{k_{p,pll}\Delta\omega_g V_g cos\delta}{1-k_{p,pll}l_g i_d}$ in $\frac{d\Delta\omega_{pll}}{dt}$ is less than the $RoCoF(t)$ in $\frac{d\Delta\omega_g}{dt}$, then the slope of the $\frac{d(\Delta\omega_{pll}-\Delta\omega_g)}{dt}$ decreases and the phase δ at its peak value increases resulting in a lower stability margin. Referring to the phase portrait of (9) in Fig. 3, the negatively increase in RoCoF shrinks the stability boundary and may lead to the loss of the synchronization. At the instant of the fault occurrence, only the grid voltage step changes while the frequency keeps unvaried due to the inertia in the power system. Hence, the initial effect of the perturbance on the phase-space trajectory of the converter is the same as that consisting in a grid voltage amplitude sag, i.e. $(\delta_{s,0}, \Delta\omega_{pll@V_g}(t_0^+))$.

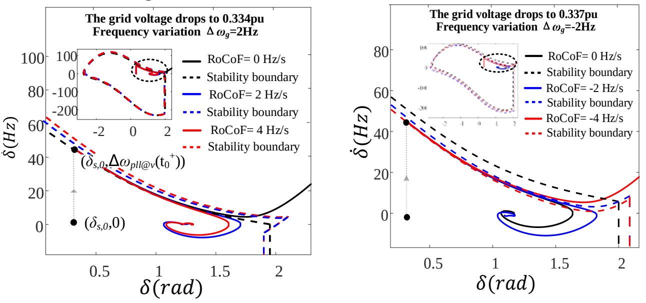

(a) grid frequency increase (b) grid frequency decrease

Fig. 3 Effect of the frequency variation.

C. Effect of combined grid voltage and frequency variations

We consider in this section combined variations of both the voltage phase and the grid frequency after a fault. In this scenario, the initial point at the instant of the fault occurrence can be obtained by substituting $(V_{g,0}+\Delta V_g)\angle((\omega_{g,0}+\Delta\omega_g)t+\theta_{g,0}+\Delta\theta_g)$ into (2), as follows:

$$\begin{cases} \Delta\delta_{pll@c}(t_0^+) = \delta_{s,0} - \Delta\theta_g, \\ \Delta\omega_{pll@c}(t_0^+) = \dfrac{k_{p,pll}(V_{g,0}+\Delta V_g)\sin(\Delta\omega_g t + \Delta\theta_g - \delta_{s,0})}{1-k_{p,pll}l_g i_d} + \\ \qquad + \dfrac{-k_{p,pll}V_{g,0}\sin(-\delta_{s,0})}{1-k_{p,pll}l_g i_d}. \end{cases} \tag{10}$$

Equation (9) shows that $\Delta\omega_{pll@c}(t_0^+)$ equals to $\Delta\omega_{pll@\theta_g}(t_0^+)+\Delta\omega_{pll@V_g}(t_0^+)$. This is because at the instant of the fault occurrence, $\Delta\omega_g(t_0^+)=0$, and the initial perturbance is only affected by the voltage magnitude change. However, from (9), it appears that the phase jump only has an impact on the initial perturbance while the grid frequency influences the transient behavior of the GFL.

Considering that the grid code restricts the frequency variation and phase-angle jump within a limited range, e.g., $\pm$ 1.5 Hz and 30° in the Chinese grid code, the effect of the grid frequency variation and phase-angle jump on the GFL transient response can be approximated in a linear process compared with that of the voltage change. Then at a given grid voltage V_g, the state space of (9) can be obtained as follows:

$$\begin{bmatrix} \Delta\dot{\theta}_{pll} \\ \Delta\dot{\omega}_{pll} \end{bmatrix} = \begin{bmatrix} 0 & 1 \\ A & B \end{bmatrix} \begin{bmatrix} \Delta\theta_{pll} \\ \Delta\omega_{pll} \end{bmatrix} + \begin{bmatrix} 0 & -1 \\ A & -B \end{bmatrix} \begin{bmatrix} \Delta\theta_g \\ \Delta\omega_g \end{bmatrix} \tag{11}$$

$$\text{Where}\begin{cases} A = -\dfrac{k_{i,pll}(V_{g,0}+\Delta V_g)cos\delta_{s,1}}{1-k_{p,pll}l_g i_d} \\ B = -\dfrac{k_{p,pll}(V_{g,0}+\Delta V_g)cos\delta_{s,1}-k_{i,pll}l_g i_d}{1-k_{p,pll}l_g i_d} \\ \delta_{s,1} = sin^{-1}\left(\dfrac{\omega_g l_g i_d + r_g i_q}{V_{g,0}+\Delta V_g}\right) \end{cases}.$$

This proves that one can decouple the combined grid disturbances into a serial of the single disturbance (i.e. grid voltage and frequency). Figure 4 compares trajectory of the phase portrait from the combined grid disturbances with the synthetic results from single disturbance, which proves the effect of the combined disturbances on the synchronization transients is the superposition of the effects of each disturbance.

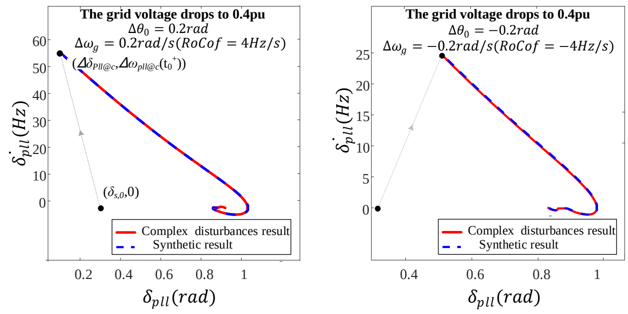

Fig.4 Effect of the superposition in combined grid disturbances

IV. Simulation Verification

This section verifies the analysis of the effect of the grid disturbances on the synchronization stability through an EMT model of a 10 kV/50 Hz GFL built in Matlab/Simulink. The line impedance is set to be 0.1 H and 1 Ω, and the PLL PI coefficient is 0.022/0.392.

A. Effect of phase-angle jumps

This case aims at validating the effect of voltage phase-angle jumps. The grid voltage sags to 0.34 pu with the phase jump at 2s. As expected, when the phase of the GFL equilibrium point is positive, a positive phase jump can enlarge the acceleration area and over amplify the PLL frequency change. In extreme cases, this effect can result in the loss of synchronization of the GFL.

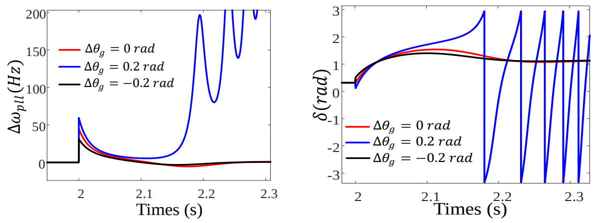

Fig. 5 Effect of the phase-angle jump.

B. Effect of grid frequency variations

This case aims at validating the effect of grid frequency variations. The grid voltage sags with the frequency variation at 2s. The grid frequency does not influence the instant change on the GFL frequency. Interestingly, the grid frequency increase helps enhance the synchronization stability, and, even more interestingly, the higher the RoCoF, the better the transient response. On the other hand, a decrease of the grid frequency has a negative impact on the synchronization stability, and the GFL becomes unstable for high values of the RoCoF.

C. *Effect of combined grid voltage and frequency variations*

This case aims at validating the use of superposition in the analysis of the effect of the combined grid disturbances on the synchronization stability. The grid voltage drops to 0.4 pu with both the phase-angle jump and the frequency change at 2 s. Figure 7 compares the result from the combined grid disturbances with the synthetic results from single disturbance. As expected, since the phase jump only affects the initial perturbance while the frequency affects the rest of the process after the initial perturbation, the GFL transients from the combined grid disturbances can be precisely represented by the transients from the separate disturbance.

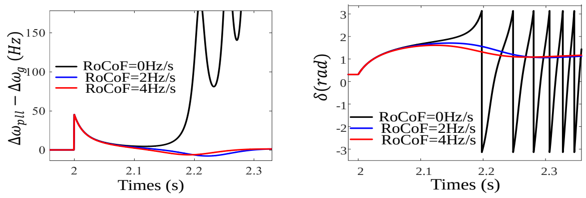

(a) The grid voltage drops to 0.334 pu and $\Delta\omega_g = 2$ Hz.

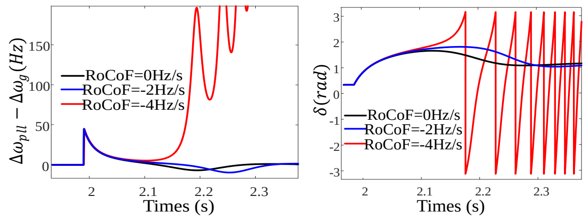

(b) The grid voltage drops to 0.337 pu and $\Delta\omega_g = -2$ Hz.

Fig. 6 Effect of the grid frequency variation.

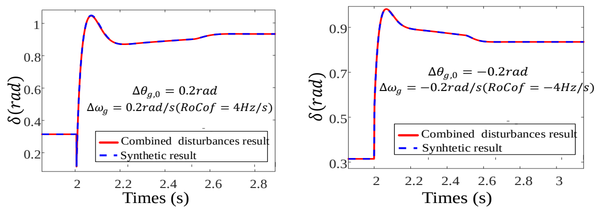

Fig. 7 Effect of the superposition in combined grid-state variation.

V. Conclusions

This letter analyzes the effect of different grid disturbances on the synchronization stability. The phase-angle jump influences the initial GFL response at the instant of the fault occurrence while the grid frequency influences the GFL following transient response after the initial perturbance and the stability boundary. The most relevant conclusions of this work are: (i) the variation of the frequency with higher RoCoF, in scenario of that makes the phase difference between the GFL and the grid reduce, is beneficial for the stability of the GFL; and (ii) the effects of the various variations of the voltage and the frequency can be studied separately, as they are either decoupled in time or superpose linearly in the model of the GFL. Based on these results, the authors are working on further enhance the synchronization stability of GFLs through the synthesis of novel controllers.

References

[1] “Performance of phase-locked loop based converters,” NationalGrid, London, U.K., Technique Report, 2017, available at www.nationalgrideso.com/document/ 102876/download.

[2] O. Goksu, R. Teodorescu, C. L. Bak, F. Iov, and P. C. Kjær,“Instability of wind turbine converters during current injection to low voltage grid faults and PLL frequency based stability solution,” *IEEE Trans Power Syst*., vol. 29, no. 4, pp. 1683–1691, Jul. 2014.

[3] M. G. Taul, X. Wang, P. Davari and F. Blaabjerg, "An overview of assessment methods for synchronization stability of grid-connected converters under severe symmetrical grid faults," in *IEEE Trans. on Power Electron.*, vol. 34, no. 10, pp. 9655–9670, Oct. 2019.

[4] D. Dong, B. Wen, D. Boroyevich, P. Mattavelli, and Y. Xue, “Analysis of phase-locked loop low-frequency stability in three-phase grid-connected power converters considering impedance interactions,” *IEEE Trans. Ind. Electron*., vol. 62, no. 1, pp. 310–321, Jan. 2015.

[5] S. Ma, H. Geng, L. Liu, G. Yang and B. C. Pal, "Grid-synchronization stability improvement of large scale wind farm during severe grid fault," *IEEE Trans. on Power Syst.*, vol. 33, no. 1, pp. 216-226, Jan. 2018.

[6] H. Wu and X. Wang, "Design-oriented transient stability analysis of PLL-synchronized voltage-source converters," *IEEE Trans. on Power Electron.*, vol. 35, no. 4, pp. 3573-3589, April 2020.

[7] J. Zhao, M. Huang, H. Yan, C. K. Tse and X. Zha, "Nonlinear and transient stability analysis of phase-locked loops in grid-connected converters," *IEEE Trans. on Power Electron*., vol. 36, no. 1, pp. 1018-1029, Jan. 2021.